A SPECTROSCOPIC COMPARISON BETWEEN HIGH- AND LOW-VELOCITY K GIANTS*

MARTIN AND BARBARA SCHWARZSCHILD,† L. SEARLE, AND A. MELTZER
Princeton University Observatory
Received July 31, 1956

ABSTRACT

High-dispersion spectra of six high-velocity and ten low-velocity K giants were taken with the coudé spectrograph of the 100-inch telescope at Mount Wilson. Central depths were measured for 78 lines and profiles for 3 lines in the region λλ 4100–4500 The high-velocity giant ϕ^2 Ori was found to deviate from the low-velocity giants in an appreciable strengthening of CH relative to Fe I, a slight weakening of CN relative to Fe I, and a weakening of the Fe I lines—all in agreement with previous estimates. The amounts of these deviations can be explained by a deficiency of the metals in ϕ^2 Ori by a factor of 4 and by a deficiency of carbon, nitrogen, and oxygen by a similar amount. The same type of deviations, though to a lesser degree, were found for the high-velocity giants 14 And and α Boo, while no significant deviations were found for HD 39853, HD 154733, and α Sct Regarding the abundance of barium and the rare earths relative to iron, no significant difference was observed between any of the high- and low-velocity giants

I. INTRODUCTION

In recent years a variety of investigations has brought forth evidence indicating that one of the basic differences between stellar populations lies in their chemical composition. Direct attempts to determine these differences in composition by high-dispersion spectrophotometry are, however, still few in number (Iwanowska 1950; Miczaika 1950; Schwarzschild 1950; Aller and Chamberlain 1951; Gratton 1953; Burbidge 1956). It is the aim of the present paper to extend these investigations further.

To make possible a tight comparison between stars belonging to different populations, it appears advantageous to select stars of as nearly the same spectral type and luminosity as practicable. For this reason the K giants were selected for this investigation, since they are represented both in population I and in population II.

The sixteen stars included in this program are listed in Table 1. They were selected mainly according to their velocity, ten of low velocity to represent population I and six of high velocity to represent population II. The space velocities, corrected for solar motion, are given in the fifth column of Table 1; in some cases they are uncertain by as much as 30 per cent. The apparent visual magnitudes, spectral types, and colors for the high-velocity stars were taken from Roman (1955) and for the low-velocity stars from Johnson and Morgan (1953). For a few low-velocity stars not found in the last source, the spectral types were taken from Roman (1952), while the colors for these stars were kindly determined by J. Schopp with the photoelectric photometer at the Princeton 23-inch refractor.

II. OBSERVATIONS

Spectrograms were obtained for all the program stars with the coudé spectrograph of the 100-inch telescope at Mount Wilson. A second-order grating and the 32-inch camera were used, giving a dispersion of 10.2 A/mm. The width of the spectrograph slit was chosen to correspond to 0.016 mm on the plate. The spectra were widened by trailing, so that they had uniform density over a width of approximately 0.2 mm on the plate. Eastman IIa-O plates were used throughout.

* This investigation was made possible by a co-operative arrangement between the Mount Wilson and Palomar Observatories and the Princeton University Observatory.

† This research was supported in part by funds of the Eugene Higgins Trust allocated to Princeton University.

The wave-length range from λ 4100 to λ 4500 was selected for this investigation. This range has the disadvantage of being rather crowded with lines but has the advantage of containing CH and CN bands, which appeared of decisive importance for the present purpose. In this wave-length range the intensity of the K giants drops so steeply toward shorter wave lengths that the whole range could not be covered by one exposure without using dangerously low or high photographic densities at the two ends. Therefore, the wave-length range was divided into two equal regions, and separate exposures were taken for each region. Two spectrograms were used for each region, making a total of four spectrograms per star or sixty-four for the entire program. The number of spectrograms actually taken was about twice as large as the number used; nearly half of the spectrograms taken were somewhat over- or underexposed. They would, therefore, have

TABLE 1

PROGRAM STARS

	Star	Bright-Star Catalogue	1900		Velocity (km/sec)	m_{vis}	Sp. Type	Color $B-V$
			α	δ				
A	δ And	165	0^h34^m	+30°	20	3 5	K3 III	1 27
B	ν Psc	489	1 36	+ 5	20	4.7	K3 III	1 34
C	α Ari	617	2 2	+23	20	2 0	K2 III	1 15
D	γ Tau	1346	4 14	+15	30	3 6	K0 III	0 99
E	δ Tau	1373	4 17	+17	30	3 7	K0 III	0 98
F	α Tau	1457	4 30	+16	40	0 8	K5 III	1 51
G	ι Aur	1577	4 50	+33	10	2 9	K3 II	1 49
H	ϕ^2 Ori	1907	5 31	+ 9	100	4 1	K0 III	0 95
I	HD 39853	2065	5 50	−12	120	5 7	K5 III	1 53
K	α Boo	5340	14 11	+20	120	0 0	K2 III	1 23
L	HD 154733	6364	17 2	+22	120	5 6	K4 III	1 30
M	α Sct	6973	18 30	− 8	100	3 8	K3 III	1 34
N	HD 173780	7064	18 42	+27	10	4 9	K3 III	1 22
O	γ Aql	7525	19 42	+10	10	2 8	K3 II	1 50
P	η Cyg	7615	19 53	+35	20	4 0	K0 III	1 04
Q	14 And	8930	23 26	+39	120	5 2	G8 III	1 02

been dangerous to use for accurate photometry of K-type spectra, with their great intensity contrasts and their obscured continua, which are difficult to define even on the best exposures (to obtain a proper photographic density, the average seeing during each exposure had to be estimated to better than ½ unit on the Mount Wilson scale, which seemed far from easy).

The observations were carried out from July to October, 1951, and during November, 1953. Each month the adjustment of the auxiliary optics which provide the calibration-step spectra was checked, and each night a special plate was taken to determine the uniformity of the illumination on the calibration steps. From these special plates, monthly small corrections for the step intensities were derived which were subsequently applied in the construction of the calibration-curves. This cautious procedure produced calibration-curves with a high internal accuracy.

The sixty-four well-exposed spectrograms were registered with the Mount Wilson microphotometer, with hundred-fold enlargement, and with the width of the photometer slit chosen to correspond to 0.007 mm on the plate. On each spectrogram the step-calibration spectra were registered twice, once at each end of the wave-length region in question.

The two calibration registrations were found to give calibration-curves so nearly alike that one mean calibration-curve was used for each spectrogram throughout its 200 A region.

All during the observations, as well as during the subsequent measurements and reductions, care was taken to avoid as much as possible any variations in instrumental conditions or techniques. Such consistency cannot reduce the external errors but may increase the internal accuracy, which is the decisive factor in the determination of differences between stars, such as are aimed for in this program.

III. FIDUCIAL CONTINUUM

Owing to the great crowding in K-type spectra, it is not possible to determine the theoretical continuum from direct measurements in the spectrogram tracings. Nor is such a determination necessary in programs like the present one, which aim not for abso-

TABLE 2

PEAKS DEFINING FIDUCIAL CONTINUUM

SHORTWARD REGION				LONGWARD REGION			
λ	δ	λ	δ	λ	δ	λ	δ
4117 2*	−0 03	4231 2	+0 05	4277 8	0 00	4378 7	+0 01
4128 5*	+ 01	4234 8	+ 05	4279 3	− 01	4386 3	+ 09
4136 2*	+ 02	4244 1	− 02	4283 6	00	4394 4	+ 05
4140 9	+ 07	4245 7	+ 01	4288 5	+ 05	4402 2	+ 01
4148 0	+ 09	4257 8	+ 03	4295 5.	+ 03	4411 6	00
4158 6	+ 08	4259 5	+ 09	4316 4*	− 02	4425 1	00
4168 2	+ 05	4266 3	00	4319 9*	+ 01	4428 9	+ 02
4171 2	+ 05	4277 8	− 02	4328 4*	+ 01	4437 2	00
4185 2	+ 06	4279 3	− 03	4332 3	+ 02	4448 7.	− 02
4189 3	+ 06	4283 6	− 01	4333 6	− 02	4451 3*	− 02
4199 6	+ 11	4288 5	+ 05	4342 8	− 01	4454 2*	+ 02
4203 3	+ 09	4295 5.	+ 01	4345 3	+ 01	4463 9*	− 01
4209 2	− 01	4316 4*	− 03	4349 7	− 02	4473 4	+ 01
4216 7	− 01	4319 9*	+ 01	4357 1	+ 02	4476 4	+ 04
4219 1	+ 02	4328 4*	+0 02	4365 2	+ 01	4483 2	+ 05
4221 8	+0 04			4370 8	+0 03	4492 9	+0 05

lute values but for differences between the program stars. Instead, it suffices to define and measure a fiducial continuum which can serve as a consistent reference line for the intensities of the absorption lines. To serve its purpose the fiducial continuum must be defined so that it can be reproduced with good accuracy throughout the range in spectral type covered by the program stars. The following procedure was used in this program.

From the tracings thirty-one peaks were selested in the shortward wave-length region and thirty-two peaks in the longward region—with eight peaks common to both regions to insure the continuity of the fiducial continuum through the entire wave-length range. The wave lengths of these peaks are listed in Table 2. For the selection of these peaks the main criteria were height and consistency from the earliest to the latest spectral types in the program.

The height of the peaks was measured on the tracings, and these measurements were transformed into intensities with the help of the calibration-curves. When these intensities were plotted against wave length for each star, it became clear that the fiducial continuum could not be simply defined by drawing a curve through the plotted points. If the curve had been drawn fairly closely through the measured points, the fiducial continuum

would have turned out rather wiggly and accordingly could not have been reproduced from star to star with sufficient consistency. If, on the other hand, the curve had been drawn smoothly through the highest points only, the fiducial continuum would have been defined only by the few highest peaks and accordingly would have been rather uncertain because of the observational errors in the individual peak measurements. These two alternative difficulties were circumvented by an intermediate step.

Near each end of each of the two wave-length regions a group of three high peaks was selected (asterisks in Table 2). Then, separately for each star and each wave-length region, a mean point was plotted for each of the two groups in the log I versus λ plot, and the two mean points were connected by a straight line. Next, the deviations of the individual peak points from this straight line were determined. Finally, an average deviation was formed for each individual peak by averaging the deviations obtained from the various stars. These average deviations, δ, are listed in Table 2, a positive sign designating a relatively low peak and a negative sign a high peak.

Now, instead of plotting directly the measured peak intensities against wave length, the measured log I values of the individual peaks were first corrected by adding the δ values given in Table 2, and the corrected log I values were then plotted against wave lengths. In these corrected plots—one for each star—the individual dots fell, of course, very close to a straight line, and the best-fitting straight line could be determined with high accuracy from a least-squares solution. The results of these least-squares solutions were accepted as the final fiducial continua to which all subsequent intensity measurements were referred.

Through the procedure just outlined, the fiducial continuum used in this investigation is completely defined by the list of peaks given in Table 2 and by the corrections to the logarithms of the measured peak intensities given in the same table.

IV. LINE DEPTHS AND PSEUDO-CURVES OF GROWTH

Seventy-eight atomic and molecular lines were selected for line-depth measurements and are listed in Table 3. Only such lines were included as appeared substantially free of blending at their centers. Molecular features were included only if a single line could be isolated or if an otherwise unblended double line had a separation so small that turbulence in the giant atmospheres would make it behave like a single line. For the selection of the lines the *Revised Rowland Tables* for the sun (St. John *et al.* 1928) as well as the table of lines for β Peg (Davis 1947) were found of great help.

The central depths of the first thirty-seven lines were measured on the tracings covering the shortward wave-length region and those of the remaining forty-one lines on the tracings covering the longward region. All these measurements were converted into intensities with the help of the calibration-curves. The results are given in Table 4 in terms of the quantity log I_C/I_L, where I_C designates the intensity of the fiducial continuum and I_L the intensity of the line center. Each entry in Table 4 gives the result for one line (numbered) of one star (lettered) and is the mean of two determinations from the two spectrograms covering the wave-length region in question for the given star. The probable error for each number in Table 4 is approximately ± 0.011 as determined from the differences between the results from the individual spectrograms.

To derive abundance ratios from the data of Table 4, curves of growth are needed. Genuine curves of growth cannot be derived here, since central line depths rather than equivalent widths were measured. However, the use of pseudo-curves of growth appropriate for the line-depth measurements does not appear to introduce any difficulties, as long as strong lines are avoided.

The pseudo-curves of growth were constructed with the help of the fifteen Fe II lines listed in Table 5 for which log S' values are available from an investigation by Bell (1951). Here S' represents a quantity proportional to the effective number of atoms in the solar atmosphere, reduced to zero excitation potential. The solar S' values were

transformed into S values appropriate to the average spectral type of the program stars with the help of the following formula:

$$\log S = \log S' - 1.25\ (\text{E.P.} - 2.28)\ .$$

The coefficient of the excitation potential in this formula was determined in a preliminary study from the condition that the few Fe I lines with very low excitation potential contained in Table 3 should fall on the same pseudo-curve of growth as the Fe I lines with average excitation potential listed in Table 5. The value thus obtained for this coefficient

TABLE 3

LIST OF LINES FOR DEPTH MEASUREMENTS

No.	λ	Element	Mult.	E.P.	No.	λ	Element	Mult	E P.
1	4128 74	Fe II	27	2 57	40	4330 02	V I	5	0 00
2	4133 44	Si H	0,0		41	4331 64	Ni I	52	1 67
3	4135 70	Si H	0,0	. .	42	4337 92	Ti II	20	1 08
4	4137 65	Ce II	2	0 04	43	4338 26	Fe I	70	2 17
5	4137 97	Fe I	320	2 82	44	4340 47	H	1	10 15
6	4138 84	Fe I	117	2 27	45	4347 24	Fe I	2	0 00
7	4139 93	Fe I	18	0 99	46	4348 34	CH	0,0	. .
8	4158 43	CN	1,2		47	4348 94	Fe I	414	2 98
9	4159 19	CN	2,3		48	4356 38	CH	0,0	
10	4162 69	CN	1,2		49	4360 81	Fe I	903	3 63
11.	4166 00	Ba II	4	2 71	50	4365 90	Fe I	415	2 98
12	4167 27	Mg I	15	4 33	51 .	4368 63	Nd II	11	0 06
13	4175 64	Fe I	354	2 83	52	4375 93	Fe I	2	0 00
14	4183 63	CN	0,1	.	53 .	4376 78	Fe I	471	3 00
15	4185 73	CN	1,2		54	4377 80	Fe I	645	3 26
16.	4186 12	Ti I	129	1 50	55	4379 24	V I	22	0 30
17	4206 21	CN	0,1	. .	56	4380 09	CH	0,0	
18	4207 13	Fe I	352	2 82	57	4386 10	CH	1,1	.
19	4211 00	CH	0,0	. .	58	4388 41	Fe I	830	3 59
20	4220 66	Sm II	15	0 18	59	4389 24	Fe I	2	0 05
21	4222 22	Fe I	152	2 44	60	4389 97	V I	22	0 27
22	4233 17	Fe II	27	2 57	61	4392 58	Fe I	973	3 86
23	4233 61	Fe I	152	2 47	62	4395 85	Ti II	61	1 24
24	4238 38	La II	41	0 40	63	4398 02	Y II	5	0 13
25	4238 82	Fe I	693	3 38	64	4399 20	Ce II	81	0 33
26	4240 70	Cr I	105	2 97	65	4410 52	Ni I	88	3 29
27	4241 68	Zr I	45	0 65	66	4417 72	Ti II	40	1 16
28	4246 83	Sc II	7	0 31	67	4419 94	V I	21	0 27
29	4250 12	Fe I	152	2 46	68	4432 57	Fe I	797	3 56
30	4250 79	Fe I	42	1 55	69	4433 22	Fe I	830	3 64
31	4252 30	Co I	1	0 10	70	4434 32	Sm II	36	0 38
32	4257 66	Mn I	23	2 94	71	4437 84	V I	21	0 29
33	4266 97	Fe I	273	2 72	72	4442 34	Fe I	68	2 19
34	4267 40	CH	0,0	. .	73	4443 80	Ti II	19	1 08
35	4281 37	Ti I	44	0 81	74	4445 48	Fe I	2	0 09
36	4287 40	Ti I	44	0 83	75	4446 39	Nd II	49	0 20
37	4292 68	Ti I	79	1 04	76	4447 72	Fe I	68	2 21
38	4317 32	Zr II	40	0 71	77	4449 14	Ti I	160	1 88
39	4322 51	La II	25	0 17	78	4453 71	Ti I	160	1 87

TABLE 4

MEASUREMENTS OF LINE DEPTHS, LOG I_c/I_L

No	A	B	C	D	E	F	G	H	I	K	L	M	N	O	P	Q
1	0 25	0 20	0 20	0 20	0 18	0 24	0 25	0 15	0 32	0 18	0 27	0 22	0 23	0 24	0 20	0 17
2	31	31	0 27	19	19	36	35	20	38	29	38	34	32	36	22	23
3	39	27	0 29	30	30	24	31	16	34	27	37	36	34	33	29	24
4	23	19	0 23	23	21	22	22	18	22	22	21	24	25	26	23	19
5	28	18	0 24	24	25	24	27	14	24	23	28	27	27	25	26	21
6	35	23	0 28	32	30	18	31	13	20	20	30	28	30	31	30	21
7	43	43	0 38	35	35	54	56	31	54	42	46	46	42	48	40	37
8	37	25	0 29	32	32	30	30	18	29	28	37	32	30	32	31	26
9	28	22	0 29	36	28	16	26	26	19	26	28	27	30	29	30	32
10	26	17	0 27	33	18	10	21	12	11	19	25	23	26	24	16	21
11	35	26	0 24	32	27	34	29	12	32	23	36	32	30	32	24	19
12	73	59	0 62	66	67	59	62	52	63	59	65	66	65	62	62	60
13	54	43	0 54	51	46	46	52	33	47	42	51	49	50	51	44	44
14	28	25	0 28	31	29	27	31	14	29	26	29	27	29	32	28	20
15	31	17	0 26	32	13	14	23	11	11	18	28	23	26	22	24	19
16	47	43	0 38	33	28	50	52	26	49	38	47	46	42	47	31	33
17	24	19	0 16	17	17	21	26	09	24	17	24	24	19	25	17	14
18	38	34	0 33	37	30	38	43	24	35	38	36	42	36	42	35	35
19	32	25	0 31	32	30	20	27	29	22	27	30	30	32	28	34	31
20	18	18	0 12	13	11	24	22	08	18	11	18	17	14	21	13	08
21	64	56	0 55	52	37	68	64	38	61	50	64	61	59	61	53	47
22	38	35	0 37	45	41	37	45	29	34	35	39	40	37	42	43	36
23	70	57	0 60	64	56	65	67	47	57	53	68	64	65	64	59	53
24	29	31	0 33	29	25	27	40	18	30	24	34	32	33	40	31	26
25	58	50	0 55	57	52	47	60	38	45	47	56	57	56	54	57	50
26	31	28	0 30	31	27	29	32	20	28	26	32	32	33	32	28	25
27	22	24	0 15	10	08	40	30	09	38	18	24	24	19	30	12	08
28	63	56	0 60	54	52	65	71	48	66	57	60	60	58	64	54	53
29	84	69	0 75	75	65	76	81	56	71	65	81	74	79	76	71	64
30			1 01		82			70	94						86	88
31	59	54	0 52	40	37	68	64	29	66	48	57	60	53	62	39	40
32	29	24	0 25	23	18	28	31	18	28	23	29	26	25	30	23	18
33	35	32	0 34	33	32	34	36	28	34	33	37	36	34	38	31	32
34	21	16	0 21	22	18	14	20	20	13	22	22	21	22	20	24	20
35	28	30	0 25	20	11	41	36	16	45	31	30	31	26	38	22	22
36	41	40	0 35	27	24	60	47	41	62	39	43	43	35	48	26	31
37	18	20	0 16	14	08	24	29	06	26	18	19	19	16	29	09	08
38	23	22	0 22	19	13	22	29	10	23	15	22	18	18	30	17	12
39.	17	20	0 16	15	12	18	26	09	19	16	15	16	17	22	12	09
40	40	44	0 33	30	25	47	50	24	50	39	39	42	35	49	28	37
41	35	33	0 28	33	28	38	44	25	34	36	32	38	32	44	29	24
42	50	53	0 44	49	44	52	67	37	51	49	49	52	48	64	43	44
43	44	43	0 37	39	34	44	49	28	44	38	41	42	37	47	33	34
44	54	65	0 66	78	69	66	84	76			56	61	68	78	68	
45	37	39	0 30	30	27	47	54	19	47	38	34	39	35	57	28	27
46	15	15	0 19	19	16	11	15	.19	14	17	14	17	20	17	14	19
47	25	20	0 22	26	22	23	30	14	22	22	23	25	23	29	22	21
48	20	18	0 20	17	18	15	17	20	20	23	18	19	16	18	17	20
49	33	33	0 29	29	27	36	40	15	39	26	32	33	27	44	24	22
50	22	24	0 18	24	26	30	28	16	26	22	19	29	26	28	28	31
51	24	21	0 19	18	14	30	29	11	27	20	22	23	21	31	14	14
52	87	83	0 72	66	54	..	..	54	..	70	79	88	74	..	62	63
53	23	26	0 20	24	19	23	28	18	25	24	22	27	26	31	20	19
54	25	25	0 24	22	17	26	28	15	25	19	21	25	23	26	18	18
55	70	61	0 51	48	41	75	70	42	72	55	63	66	55	71	44	47
56	29	24	0 26	26	22	24	29	23	23	25	23	29	25	30	24	25
57	22	17	0 19	18	15	21	21	18	17	18	20	20	21	22	16	16
58	48	38	0 35	44	35	40	51	26	32	34	40	45	42	47	37	32
59	51	48	0 43	40	33	55	66	31	58	50	46	55	44	70	34	36
60	69	63	0 61	55	46	74	72	42	70	56	65	70	57	74	53	53
61	23	18	0 20	21	17	17	23	14	16	16	19	23	21	21	19	14
62	30	32	0 33	31	28	32	43	24	38	33	27	35	31	44	30	27
63	34	34	0 29	27	23	40	44	21	43	33	31	36	30	45	25	23
64	0 22	0 26	0 21	0 20	0 18	0 28	0 34	0 17	0 28	0 18	0 22	0 26	0 23	0 35	0 18	0 14

TABLE 4—*Continued*

No	A	B	C	D	E	F	G	H	I	K	L	M	N	O	P	Q
65	0 24	0 26	0 33	0 28	0 24	0 25	0 34	0 16	0 23	0 21	0 26	0 27	0 24	0 32	0 21	0 20
66	38	39	0 37	39	34	39	54	33	46		37	42	38	49	33	35
67	44	34	0 29	23	20	41	43	12	41	..	36	38	29	42	19	18
68	22	19	0 22	23	18	19	29	15	23	16	21	22	23	26	19	18
69	45	40	0 37	39	38	38	50	30	39	37	43	42	42	50	37	32
70	39	34	0 30	30	27	39	44	19	37	32	37	38	33	45	29	22
71	48	47	0 38	32	29	55	58	24	55	45	46	51	40	60	32	29
72	76	78	0 63	65	57	77	84	47	69	63	69	79	66	81	68	54
73	55	49	0 46	51	43	54	61	34	55	46	51	57	49	60	46	44
74	36	36	0 31	28	22	42	52	18	45	35	33	43	32	55	24	27
75	16	21	0 18	19	12	25	33	12	24	29	17	20	19	29	16	13
76	71	60	0 62	62	50	67	72	44	59	57	63	70	60	73	54	49
77	34	36	0 28	30	25	40	48	25	43	31	35	38	31	45	30	27
78	0 39	0 31	0 30	0 22	0 22	0 39	0 44	0 19	0 40	0 33	0 33	0 35	0 31	0 41	0 23	0 25

corresponds to an excitation temperature of 4000°, much as one would have expected for the average spectral type of the program stars (Koelbloed 1953).

The lines of Table 5 were then divided into five groups according to their strength, and an average log S value was formed for each group. Only these five average log S values, given in the last column of Table 5, were used in the construction of the pseudo-curves of growth. It may be noted that the average excitation potentials for the five groups of lines differ from the over-all average by less than $\frac{1}{2}$ volt. This had the convenient consequence that a moderate error in the coefficient of the excitation potential in the transformation equation could not have serious effects and that the differences in the excitation temperature between the different program stars did not have to be taken into account at this point.

The pseudo-curve of growth for each star was then constructed by forming the average log I_C/I_L value for each of the five groups of Fe I lines listed in Table 5 from the data of Table 4, by plotting these averages against the average log S values given in Table 5, and by drawing a smooth curve through these five normal points. With the help of these pseudo-curves of growth each individual line-depth measurement of Table 4 could be transformed into a log S value. The results are given in Table 6.

TABLE 5

GROUPS OF Fe I LINES FOR PSEUDO-CURVES OF GROWTH

No.	log S'	E P.	log S	⟨E P⟩	⟨log S⟩
29	4 91	2 46	4 68	2 33	4 66
72	4 53	2 19	4 64		
21	4 25	2 44	4 05		
23	4 62	2 47	4 38	2 37	4 29
76	4 34	2 21	4 43		
7	2 08	0 99	3 69		
13	4 08	2 83	3 39	2 40	3 59
25	5 06	3 38	3 68		
18	3 70	2 82	3 02		
33	3 67	2 72	3 12	3 04	3 12
58	4 87	3 59	3 23		
47	3 58	2 98	2 70		
50	3 14	2 98	2 26	3 20	2 35
54	3 26	3 26	2 03		
68	4 02	3 56	2 42		

TABLE 6

LOG S VALUES DERIVED FROM LINE DEPTHS

No	A	B	C	D	E	F	G	H	I	K	L	M	N	O	P	Q
1	2 40	2 28	2 30	2 18	2 22	2 35	2 04	2 35	2 90	2 28	2 66	2 16	2 30	2 14	2 36	2 12
2	2 70	2 88	2 72	2 06	2 28	3 00	2 68	2 70	3 22	2 72	3 12	2 88	2 86	2 82	2 42	2 42
3	3 04	2 64	2 82	2 76	2 98	2 35	2 48	2 40	3 02	2 62	3 06	2 94	2 98	2 68	2 80	2 51
4	2 32	2 20	2 42	2 30	2 38	2 23	1 82	2 52	2 24	2 42	2 34	2 30	2 44	2 24	2 46	2 22
5	2 56	2 16	2 52	2 40	2 64	2 35	2 22	2 28	2 40	2 44	2 70	2 50	2 58	2 18	2 62	2 31
6	2 84	2 38	2 76	2 88	2 98	2 03	2 48	2 22	2 14	2 38	2 78	2 54	2 74	2 58	2 86	2 31
7	3 26	3 60	3 30	3 00	3 26	3 79	3 66	3 42	3 86	3 50	3 46	3 44	3 32	3 50	3 39	3 34
8	2 98	2 50	2 82	2 88	3 12	2 69	2 42	2 52	2 72	2 66	3 06	2 76	2 74	2 64	2 92	2 61
9	2 56	2 34	2 82	3 06	2 86	1 97	2 10	3 03	2 00	2 56	2 70	2 50	2 74	2 46	2 86	3 03
10	2 44	2 12	2 72	2 94	2 22	1 79	1 72	2 19	1 60	2 32	2 56	2 20	2 50	2 14	2 12	2 31
11	2 84	2 54	2 52	2 88	2 80	2 94	2 34	2 19	2 90	2 44	3 00	2 76	2 74	2 64	2 53	2 22
12	4 46	4 26	4 30	4 52	. . .	4 00	3 88	4 75	4 26	4 52	4 26	4 24	4 42	4 08	4 42	4 71
13	3 68	3 60	3 94	3 88	3 98	3 52	3 48	3 57	3 58	3 50	3 62	3 52	3 72	3 62	3 55	3 70
14	2 56	2 50	2 76	2 82	2 92	2 52	2 48	2 28	2 72	2 56	2 74	2 50	2 68	2 64	2 75	2 31
15	2 70	2 12	2 62	2 88	2 01	1 92	1 88	2 16	1 60	2 28	2 70	2 20	2 50	1 98	2 53	2 22
16	3 42	3 60	3 30	2 94	2 86	3 70	3 48	3 03	3 66	3 30	3 46	3 44	3 32	3 40	2 92	3 10
17	2 38	2 20	1 92	1 92	2 16	2 16	2 10	2 08	2 40	2 26	2 52	2 30	2 04	2 18	2 16	2 01
18	3 04	3 12	3 06	3 14	2 98	3 16	3 12	2 93	3 02	3 30	3 00	3 18	3 04	3 12	3 11	3 18
19	2 74	2 50	2 94	2 88	2 98	2 16	2 22	3 27	2 24	2 62	2 78	2 66	2 86	2 40	3 11	2 96
20	2 14	2 16			1 95	2 35	1 82	2 04	1 90		2 18			1 88	2 01	1 80
21	4 14	4 14	4 04	3 88	3 42	4 36	4 00	3 93	4 26	4 10	4 26	4 06	4 08	4 08	4 05	3 94
22	3 04	3 12	3 24	3 58	3 68	3 07	3 20	3 27	3 02	3 04	3 12	3 12	3 12	3 12	3 55	3 26
23	4 28	4 14	4 16	4 52	4 46	4 23	4 16	4 48	3 98	4 24	4 40	4 24	4 42	4 22	4 28	4 37
24	2 60	2 88	3 06	2 70	2 64	2 52	2 98	2 52	2 78	2 50	2 96	2 76	2 92	3 04	2 92	2 61
25	3 88	3 96	4 04	4 12	4 20	3 52	3 78	3 93	3 50	3 84	3 84	3 82	3 96	3 72	4 16	4 20
26	2 70	2 70	2 88	2 82	2 80	2 63	2 54	2 70	2 66	2 56	2 88	2 76	2 92	2 64	2 75	2 56
27.	2 28	2 44	. . .	. . .	1 83	3 22	2 42	2 08	3 22	2 28	2 52	2 30	2 04	2 52	1 98	1 80
28	4 00	4 14	4 16	4 00	4 20	4 23	4 32	4 60	4 44	4 38	3 96	3 94	4 08	4 22	4 04	4 37
29	4 94	4 54		5 00	5 01	4 64	4 66	5 11	5 10	4 82		4 64		4 66	4 89	5 25
30																
31	3 88	4 04	3 82	3 30	3 42	4 36	4 00	3 27	4 44	3 98	3 84	3 94	3 84	4 08	3 32	3 51
32	2 60	2 44	2 56	2 30	2 22	2 58	2 48	2 52	2 66	2 44	2 74	2 40	2 44	2 52	2 46	2 17
33	2 84	2 96	3 12	2 94	3 12	2 94	2 76	3 21	3 02	2 96	3 06	2 94	2 98	2 96	2 92	3 03
34	2 24	2 11	2 30	2 26	2 22	1 92	1 72	2 70	1 66	2 42	2 42	2 06	2 26	1 88	2 53	2 31
35	2 56	2 82	2 56	2 18	1 95	3 30	2 76	2 40	3 50	2 82	2 78	2 72	2 50	2 96	2 42	2 38
36	3 20	3 44	3 12	2 58	2 59	4 00	3 28	4 13	4 26	3 30	3 30	3 26	2 98	3 50	2 62	2 96
37	2 14	2 28	1 92	. . .	1 83	2 35	2 34	1 92	2 50	2 28	2 24	1 94	. . .	2 46	1 87	1 80
38	2 32	2 36	2 38	2 06	2 01	2 23	2 36	2 12	2 28	2 20	2 42		1 96	2 52	2 16	1 95
39	2 11	2 28	1 94		1 98	2 03	2 12	2 08	2 00	2 22				1 98	1 98	1 84
40	3 12	3 62	3 06	2 76	2 64	3 52	3 46	2 93	3 78	3 30	3 12	3 18	2 98	3 50	2 75	3 34
41	2 84	3 04	2 76	2 94	2 86	3 16	3 12	2 98	3 02	3 12	2 88	3 06	2 86	3 22	2 80	2 51
42	3 58	4 06	3 50	3 78	3 77	3 70	4 16	3 83	3 78	3 98	3 54	3 58	3 64	4 22	3 55	3 70
43	3 28	3 62	3 24	3 22	3 26	3 37	3 38	3 21	3 42	3 30	3 24	3 18	3 12	3 40	3 04	3 18
44	3 68	4 46	4 46	5 00		4 23	4 66				3 84	4 06	4 66	4 66	4 75	
45	2 98	3 36	2 88	2 76	2 80	3 52	3 56	2 58	3 58	3 30	2 96	3 06	2 98	3 84	2 75	2 72
46	. . .	2 09	2 18	2 06	2 12	1 83	. . .	2 58	. . .	2 26	. . .	. . .	2 16	. . .	2 04	2 22
47	2 40	2 28	2 38	2 50	2 46	2 24	2 42	2 28	2 24	2 42	2 42	2 34	2 30	2 46	2 42	2 31
48	2 24	2 18	2 30	1 92	2 22	1 95	1 62	2 70	2 14	2 44	2 18	1 94	1 80	1 62	2 16	2 31
49	2 78	3 04	2 82	2 70	2 80	3 00	2 98	2 35	3 22	2 56	2 88	2 82	2 58	3 22	2 53	2 38
50	2 28	2 44	2 08	2 40	2 69	2 69	2.28	2 40	2 50	2 42	2 24	2 60	2 50	2 40	2 75	2 96
51	2 36	2 28	2 18	1 98	2 04	2 69	2 36	2 16	2 62	2 36	2 42	2 20	2 16	2 58	2 04	2 01
52	. . .	4 88	4 94	4 52	4 32	. . .	. . .	4 91	. . .	4 98	4 96	. . .	5 00	. . .	4 42	4 98
53	2 32	2 54	2 30	2 40	2 28	2 24	2 28	2 52	2 46	2 50	2 42	2 50	2 50	2 58	2 36	2 22
54	2 40	2 48	2 52	2 26	2 16	2 44	2 28	2 35	2 46	2 32	2 34	2 34	2 30	2 24	2 22	2 17
55	4 28	4 36	3 82	3 78	3 68	4 64	4 16	4 13	5 14	4 38	4 08	4 24	3 96	4 50	3 55	3 94
56	2 60	2 44	2 62	2 50	2 46	2 35	2 36	2 83	2 28	2 52	2 42	2 60	2 44	2 52	2 53	2 56
57	2 28	2 14	2 18	1 98	2 08	2 16	1 72	2 52	1 80	2 28	2 34	2 06	2 16	1 98	2 12	2 08
58	3 50	3 36	3 12	3 48	3 26	3 22	3 46	3 03	2 90	3 04	3 18	3 34	3 32	3 40	3 25	3 03
59	3 58	3 86	3 50	3 30	3 18	3 90	4 02	3 42	4 12	4 10	3 46	3 82	3 38	4 36	3 11	3 26
60	4 28	4 36	4 30	4 12	3 98	4 50	4 32	4 13	4 66	4 38	4 24	4 42	3 96	4 50	4 05	4 37
61	2 32	2 16	2 30	2 18	2 16	1 99	1 88	2 28	. . .	2 24	2 24	2 20	2 18	1 88	2 27	2 01
62	2 64	2 96	3 06	2 82	2 86	2 82	3 12	2 93	3 22	2 96	2 66	2 88	2 80	3 22	2 86	2 72
63	2 84	3 12	2 82	2 58	2 50	3 22	3 12	2 70	3 42	2 96	2 82	2 94	2 74	3 30	2 58	2 42
64	2 28	2 54	2 30	2 18	2 22	2 58	2 68	2 32	2 66	2 28	2 42	2 40	2 30	2 76	2 22	2 01

TABLE 6—*Continued*

No	A	B	C	D	E	F	G	H	I	K	L	M	N	O	P	Q
65	2 38	2 54	3 06	2 64	2 59	2 40	2 68	2 40	2 28	2 38	2 58	2 50	2 40	2 64	2 36	2 31
66	3 04	3 36	3 24	3 22	3 26	3 16	3 56	3 57	3 58	3 72	3 06	3 18	3 18	3 50	3 04	3 18
67	3 26	3 12	2 82	2 30	2 38	3 29	3 12	2 19	3 34	2 76	3 00	3 06	2 68	3 12	2 27	2 17
68	2 28	2 20	2 38	2 30	2 22	2 08	2 34	2 35	2 28	2 24	2 34	2 16	2 30	2 24	2 27	2 17
69	3 34	3 44	3 24	3 22	3 50	3 16	3 48	3 35	3 22	3 22	3 30	3 18	3 32	3 62	3 25	3 03
70	3 04	3 12	2 88	2 76	2 80	3 16	3 12	2 58	3 14	2 88	3 06	3 06	2 92	3 30	2 80	2 38
71	3 50	3 78	3 30	2 88	2 92	3 90	3 78	2 93	3 98	3 72	3 46	3 58	3 24	3 96	2 98	2 83
72	4 66	4 76	4 30	4 52	4 46	4 64	4 66	4 48	4 66	4 66	4 40	5 08	4 42	4 82	4 75	4 37
73	3 78	3 86	3 64	3 88	3 77	3 79	3 88	3 66	3 98	3 84	3 62	3 82	3 64	3 96	3 74	3 70
74	2 92	3 20	2 94	2 64	2 46	3 29	3 48	2 52	3 50	3 04	2 92	3 26	2 86	3 84	2 53	2 72
75	2 08	2 28	2 08	2 06	1 98	2 40	2 62	2 19	2 40	2 72	2 12	2 06	2 04	2 46	2 12	1 98
76	4 46	4 26	4 30	4 38	4 20	4 36	4 32	4 24	4 12	4 38	4 08	4 42	4 08	4 48	4 05	4 07
77	2 84	3 20	2 76	2 76	2 64	3 22	3 38	2 98	3 42	2 82	2 96	3 06	2 80	3 30	2 86	2 72
78	3 04	2 88	2 88	2 26	2 46	3 16	3 12	2 58	3 28	2 96	2 92	2 88	2 80	3 12	2 46	2 56

Before the log S values could be used for the investigation of relative abundances, one further check was necessary. The line-depth measurements are based on a fiducial continuum. If this fiducial continuum runs parallel to the theoretical continuum—in terms of log I—then all the line-depth data of Table 4 need just a constant correction. This constant correction would shift the pseudo-curves of growth in the vertical direction without changing their form and the log S values of Table 6 would be completely unaffected. If, however, the fiducial continuum was more depressed relative to the theoretical continuum on one end of the wave-length range covered than on the other, then the line-depth measurements and consequently the log S values would require a wave-length-dependent correction. The possible existence of such a wave-length-dependent correction was investigated by plotting the difference between the log S values of Table 6 and the solar log S' values against wave lengths. This plot, carried out for the average of the program stars, did not show any significant wave-length dependence. This check therefore indicates that the fiducial continuum defined by the data of Table 2 runs substantially parallel to the theoretical continuum—which may not be too surprising in view of the relatively short wave-length range covered. In consequence, the log S values of Table 6 may be used as they stand.

TABLE 7

GROUPS OF ELEMENTS AND LINE NUMBERS FOR FORMATION OF AVERAGE LOG S VALUES

Fe I	5, 6, 18, 33, 43, 47, 49, 50, 53, 54, 58, 68, 69
Fe I (low E.P.)	45, 59, 74
Ti I	16, 35, 36, 77, 78
Ti II	42, 62, 66, 73
V I	40, 55, 60, 67, 71
Cr I, Mn I, Co I, Ni I	26, 31, 32, 41, 65
Ba II, La II, Ce II, Nd II, Sm II	4, 11, 24, 51, 64, 70, 75
CN	8, 9, 10, 14, 15, 17
CH	19, 34, 48, 56, 57

For the determination of relative abundances, individual lines could not safely be used because of the large observational errors of the individual log S values. Instead, groups of lines had to be used for which average log S values could be formed. The line groups here used are listed in Table 7. Each of these groups contains all the measured lines of the elements in question with the exception of those lines for which log S values could not be derived for one or more program stars. A further exception was seven strong Fe I lines which were not included in the first group so as to make the average line strength of

the first group comparable to those of the other groups. All groups contain five or more lines, with the exception of the second group (low-excitation Fe I, three lines) and the fourth group (ionized titanium, four lines).

The average log S values for the nine groups of lines and the sixteen program stars are given in Table 8, which contains the final results from the line-depth measurements. We shall discuss them in Section VI.

V. LINE PROFILES AND EQUIVALENT WIDTHS

In addition to the line depths discussed in the preceding section, line profiles were measured, however, for only three lines. The three lines selected were the weak Fe I lines 47, 68, and 74. They appeared to be the best choice regarding lack of blending that could be found.

TABLE 8

AVERAGE LOG S VALUES

Star	Fe I	Fe I Low E.P.	Ti I	Ti II	V I	Cr I etc.	Ba II etc.	CN	CH
A	2 76	3 16	3 01	3 26	3 69	2 88	2 50	2 60	2 42
B	2 77	3 47	3 19	3 56	3 85	2 95	2 55	2 30	2 27
C	2 73	3 11	2 92	3 36	3 46	3 02	2 49	2 61	2 47
D	2 76	2 90	2 54	3 42	3 17	2 80	2 41	2 75	2 31
E	2 80	2 81	2 50	3 42	3 12	2 78	2 41	2 55	2 39
F	2 69	3 57	3 48	3 37	3 97	3 03	2 65	2 18	2 11
G	2 73	3 69	3 20	3 68	3 77	2 96	2 56	2 12	1 93
H	2 65	2 84	3 02	3 50	3 26	2 77	2 35	2 38	2 80
I	2 71	3 73	3 62	3 64	4 18	3 01	2 68	2 17	2 02
K	2 70	3 48	3 04	3 62	3 71	2 90	2 51	2 44	2 46
L	2 76	3 11	3 08	3 22	3 58	2 98	2 62	2 71	2 43
M	2 74	3 38	3 07	3 36	3 70	2 93	2 51	2 41	2 26
N	2 74	3 07	2 88	3 32	3 36	2 89	2 50	2 53	2 30
O	2 80	4 01	3.26	3 72	3 92	3 02	2 72	2 34	2 08
P	2 74	2 80	2 66	3 30	3 12	2 74	2 44	2 56	2 49
Q	2 64	2 90	2 74	3 32	3 33	2 61	2 20	2 42	2 44

In each of these lines five points were measured on each tracing, with a distance between neighboring points of 0.5 mm on the tracings or 0.005 mm on the plates. These measurements were transformed into intensities with the help of the calibration-curves, the intensities were subtracted from those of the fiducial continuum, and the six measured profiles (two tracings for each of three lines) were combined into one average profile for each star. These average profiles were found to be well representable by error-curves, and the dispersion was determined for each star by a least-squares solution. The resulting values for the dispersion differed from star to star by not more than would be expected from their probable errors. These differences were therefore ignored, and the over-all average of the dispersion was formed. It turned out to be

$$\sigma = \pm 0.011 \text{ mm} = \pm 0.11 \text{ A} = \pm 8 \text{ km/sec}.$$

The instrumental profile was not determined in this program. Nevertheless, it seems safe to conclude from the slit width used (0.016 mm on plate) and from the resolution of the plate type employed that the dispersion of the measured profile as given here is

largely caused by the instrumental profile rather than by the actual profile of the stellar lines. This gives the incidental result that the over-all turbulent velocities in the atmospheres of early K giants, as represented by our program stars, must be appreciably less than 8 km/sec.

The main result of the profile measurements is the following formula, which permits the derivation of equivalent widths from the measured line depths. If one accepts an error-curve with the foregoing value of the dispersion for the profile of the weaker lines in all the program stars, one obtains for the relation between the equivalent width, W, and the central line depth,

$$W = 0.283 \times \frac{I_C - I_L}{I_C}.$$

This formula will give too small W values, if the fiducial continuum lies noticeably below the theoretical continuum, since in this case σ as well as the line depth will have been underestimated. However, this error is not likely to affect the comparison between stars, since it probably does not vary seriously from star to star.

This formula has been applied to a group of five weak Fe I lines. The lines selected are Nos. 47, 53, 54, 61, and 68. They are the five weakest Fe I lines for which the depths

TABLE 9

AVERAGE EQUIVALENT WIDTHS OF FIVE WEAK Fe I LINES

Star	$\overline{W}$	Star	$\overline{W}$	Star	$\overline{W}$	Star	$\overline{W}$
A	0 119	E	0 099	I	0 113	N	0 117
B	111	F	111	K	102	O	130
C	111	G	133	L	109	P	103
D	0 117	H	0 083	M	0 122	Q	0 096

could be measured in all program stars, excluding those with near-zero excitation potentials. Their average excitation potential is 3.3 volts. For these lines the average of the five log I_C/I_L values given in Table 4 was formed for each star, and the corresponding equivalent width was computed with the help of the formula. The results are given in Table 9. We shall discuss them in the following section.

VI. DISCUSSION OF MEASUREMENT

The data deduced from the line-depth measurements and the profile measurements are given in Tables 8 and 9, respectively. To start with Table 8, the log S values there listed have an arbitrary zero point. Hence only differences between log S values should be considered. The difference between two log S values corresponding to two elements in the same star is directly proportional to the abundance ratio of the two elements but also depends on the temperature and the pressure. Accordingly, the log S differences have to be studied in relation to color (as substitute for temperature) and luminosity class (as substitute for pressure). This may be done with the help of Figure 1.

In this figure various log S differences are plotted against the color index $B-V$. In each of the eight graphs the sixteen lettered symbols correspond to the sixteen program stars listed in Table 2. The two top graphs show the degree of excitation of iron and the degree of ionization of titanium, respectively, while the remaining six graphs show the abundance of various molecules and atoms relative to iron.

The eight dots in each graph of Figure 1 represent low-velocity giants. In all eight graphs they fall comfortably close to a smooth curve, indicating a satisfactory accuracy of the log S differences. In the first graph the steep rise of the dots with increasing color

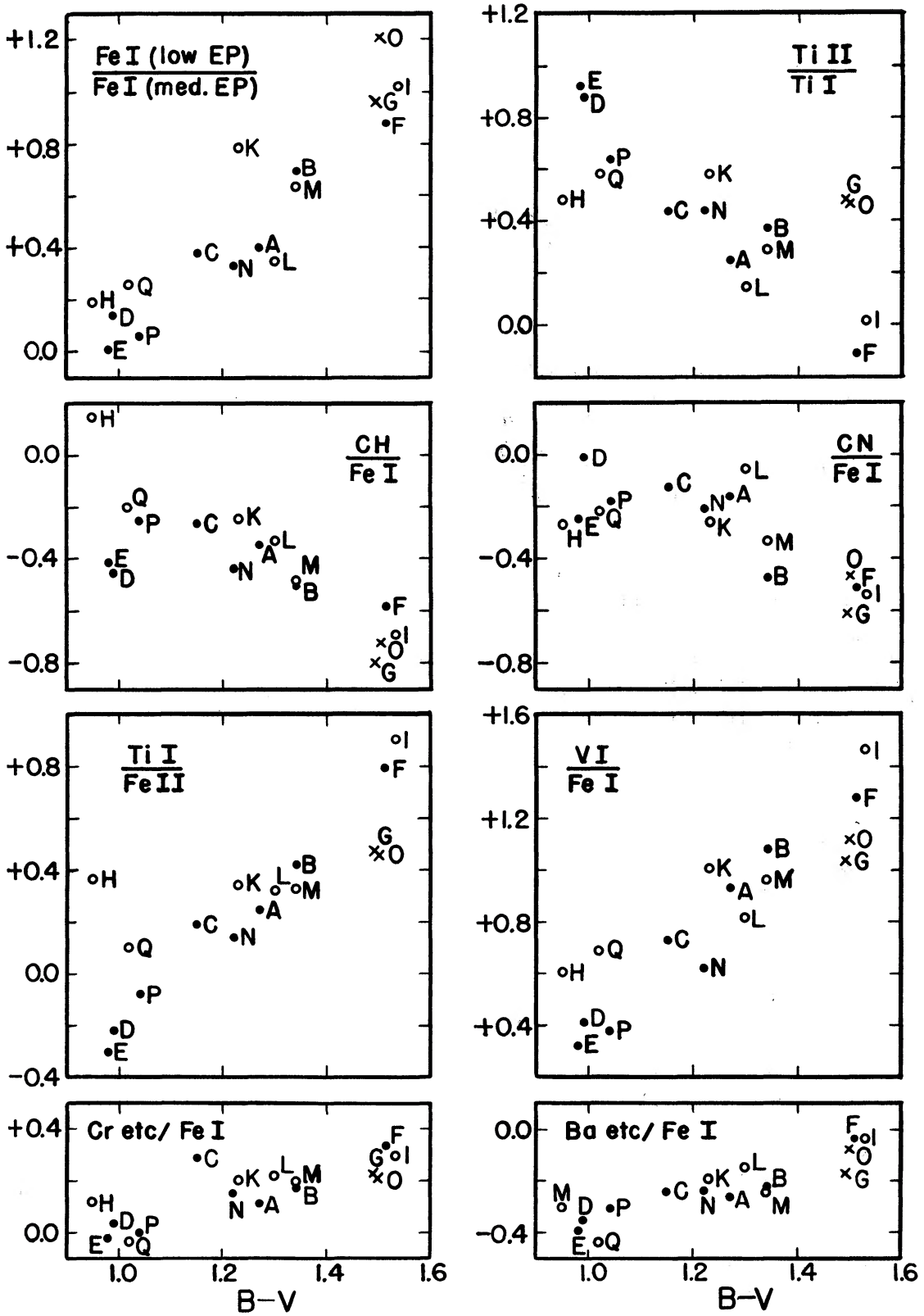

FIG. 1.—Abundance ratios for various elements. The abscissa gives the color index $B - V$, the ordinate the quantity log [S (first element)/S (second element)] Dots represent low-velocity giants; crosses, low-velocity supergiants; and circles, high-velocity giants.

index corresponds well with the decreasing excitation temperature. The low-excitation lines (second group of Table 7) have an average excitation potential of 0.05 volts, while the medium-excitation lines (first group of Table 7) have an average excitation potential of 3.03 volts. This difference of 3 volts produces, according to the first graph, a variation in the log S difference of 0.8 from K0 ($B - V = 1.0$) to K5 ($B - V = 1.5$). This corresponds to a variation in θ of 0.27, in satisfactory agreement with the usual temperature scale. The dots in the second graph show a steep drop with increasing color index, corresponding to decreasing ionization with decreasing temperature. The second and third graphs for CH and CN show the well-known shallow maxima of these bands at K1 ($B - V = 1.1$). The dots in the fifth and sixth graphs for titanium and vanadium show again a steep increase from K0 to K5. This appears to be caused by the circumstance that iron is largely neutral throughout this range in spectral type, while titanium and vanadium, with their lower ionization potentials, are still partially ionized at K0. Finally, the last two graphs show very little variation in the dots, corresponding to the circumstance that the elements in question vary little in their ionization state throughout the temperature range considered.

For the two low-velocity supergiants, represented by crosses, Figure 1 shows significant differences against the ordinary giants only in three graphs, the second, fifth, and sixth. The difference in the second graph clearly represents the fact that the lower pressure in the atmospheres of the supergiants increases the degree of ionization. The differences in the fifth and sixth graphs may be caused by two effects. First, the crowding of the lines in the blue is stronger in the supergiants than in the giants, so that the supergiants may appear redder than giants of the same temperature. Second, titanium and vanadium may still be partially ionized in K3 supergiants. Thus the low-velocity giants and supergiants behave in an understandable manner throughout Figure 1 and, in consequence, form a good standard of comparison for the high-velocity giants, a comparison which is the main aim of this program.

Of the six high-velocity giants, represented by circles in Figure 1, only star H (ϕ^2 Ori) shows significant deviations from the low-velocity giants in several graphs. It shows the well-known strengthening of CH and a slight weakening of CN. In addition, it shows significant deviations in the second graph as well as in the fifth and the sixth.

Of the remaining five high-velocity giants, stars Q and K (14 And and α Boo) show nearly consistently small deviations in the same direction as star H, while stars L, M, and I show no significant systematic deviations from the low-velocity giants. Accordingly, we shall concentrate our attention on star H, with the understanding that the same results, though to a lesser degree, probably hold for stars Q and K.

Before the main results—the strengthening of CH and the weakening of CN—can be interpreted, the deviations of star H in the second, fifth, and sixth graphs have to be explained. These three deviations all have the opposite sign from the deviations shown by the two supergiants and hence could be explained in terms of an increased electron pressure. This explanation leads, however, to results contrary to those of previous investigations and contrary to those derived below from the CH and CN measurements. The following alternative explanation appears preferable. The existence of the absorption lines will, in general, increase the color index of a star, since their over-all absorption effect is for most spectral types larger in the blue region than in the visual region. This reddening effect of the absorption lines will be smaller in population II stars than in population I stars, since the former tend to have weaker lines than the latter. Hence a positive correction has to be applied to the colors of population II stars if the corrected colors are to be equal to those of population I stars with the same temperature. This correction was recently estimated for F-type subdwarfs to amount to about 0.1 (Schwarzschild, Searle, and Howard 1955). The corresponding correction for K-type stars must be much larger than that for F-type stars, owing to the much greater strength and frequency of absorption lines. If one applies to star H a color correction of, say, 0.2 and

shifts it accordingly to the right in all graphs of Figure 1, one finds that star H fits well on the curves for the ordinary giants in the four graphs with steep slopes (first, second, fifth, and sixth) but that the deviations of star H in the graphs for the CH and CN bands are practically unaffected by this shift. We thus conclude that the only significant deviations shown by star H in Figure 1 are those found for CH and for CN. The amounts of these two deviations may be estimated from the graphs to be

$$\Delta \log \frac{S\,(\mathrm{CH})}{S\,(\mathrm{Fe\,I})} = +0.5\,, \qquad \Delta \log \frac{S\,(\mathrm{CN})}{S\,(\mathrm{Fe\,I})} = -0.1\,. \tag{1}$$

One more result can be taken from Figure 1. The last graph of this figure shows that star H does not deviate significantly from the ordinary giants in the ratio of the heaviest elements—barium and the rare earths—to iron:

$$\Delta \log \frac{S\,(\mathrm{Ba,\ etc.})}{S\,(\mathrm{Fe\,I})} = 0.0\,. \tag{2}$$

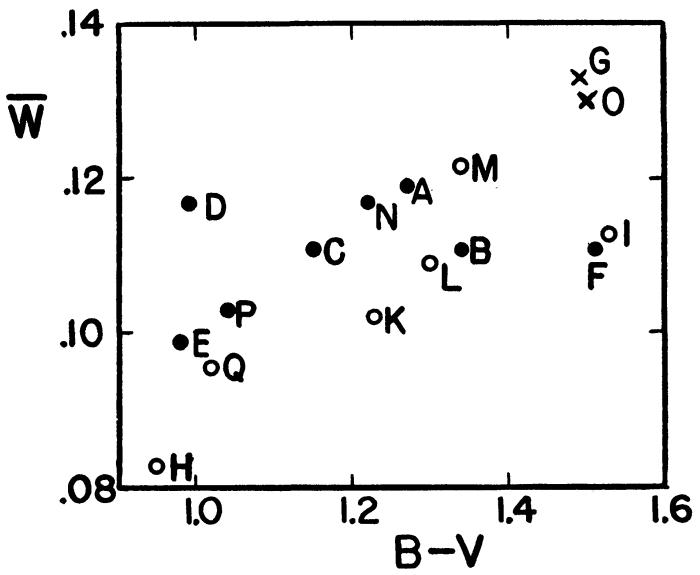

FIG. 2 —Average equivalent width (in Angstrom) of five weak Fe I lines as function of color (symbols as in Fig. 1).

To these results from the line-depth measurements, the profile measurements add one more. The average equivalent widths of weak Fe I lines, as listed in Table 9, are plotted in Figure 2 against the color index. This figure, much like the graphs in Figure 1, shows the dots which represent the low-velocity giants falling satisfactorily close to a smooth curve. The two low-velocity supergiants, represented by crosses, show stronger equivalent widths than the giants, which may be explained by the fact that the lower electron pressure in the supergiants produces a lower continuous absorption by H^-. Regarding the high-velocity giants, represented by circles, again only star H shows a strong deviation. Stars Q and K, as before, show a small deviation in the same direction as star H, while L, M, and I do not show any significant deviations from the low-velocity giants. Concentrating again on star H alone, one may estimate the deviation from Figure 2 to amount to

$$\Delta \log W = -0.1\,.$$

Since the equivalent width of weak Fe I lines depends only on the abundance ratio of Fe I to H^-, the latter providing the continuous absorption, as long as differences in the turbulent velocities are assumed to be negligible and since the slope of the curves of growth for the relevant line strength is approximately one-third, we may conclude that

$$\Delta \log \frac{S(\text{Fe I})}{S(H^-)} = -0.3 . \tag{3}$$

Equations (1), (2), and (3) represent the four main data deducible from our measurements.

VII. INTERPRETATION OF DATA

Following an earlier investigation (Schwarzschild, Spitzer, and Wildt 1951), one may interpret the results for star H, summarized in equations (1), (2), and (3), in terms of the abundance ratios A and B. Here, according to Strömgren, A represents the ratio of hydrogen to the metals (by number of atoms) and B the ratio of hydrogen to the oxygen group (including mainly carbon, nitrogen, and oxygen).

To derive the relations between the partial pressures of the observed atoms and molecules, on the one hand, and the two abundance ratios A and B, on the other hand, one has to answer two questions regarding the circumstances in the atmosphere of star H: first, Are the most abundant metals such as iron mostly neutral or mostly ionized? and, second, Are carbon and nitrogen mostly free or mostly bound in CO and N_2? According to the earlier investigation already mentioned, one would estimate for star H that the more abundant metals are mostly neutral and, second, that carbon and nitrogen are mostly bound. The first item appears fairly certain, but the second item does not now appear so sure, since star H—even after increasing its color index by 0.2—does not yet fall into the right-hand halves of the third and fourth graphs of Figure 1, where the steep dropping of CH and CN indicates the effect of the binding of carbon and nitrogen in the unobserved molecules CO and N_2. In consequence, we shall here distinguish two cases according to the state of carbon and nitrogen. The analysis described in detail in the previous investigation (Schwarzschild, Spitzer, and Wildt 1951) gives the following relations between the relevant partial pressures and the abundance ratios for the two cases:

Case 1 (metals mostly neutral, carbon and nitrogen mostly bound):

$$\frac{p_{\text{CH}}}{p_{\text{Fe I}}} \propto A , \qquad \frac{p_{\text{CN}}}{p_{\text{Fe I}}} \propto \frac{A^{5/6}}{B^{1/2}} , \qquad \frac{p_{\text{Fe I}}}{p_{H^-}} \propto \frac{1}{A^{2/3}} . \tag{4}$$

Case 2 (metals mostly neutral, carbon and nitrogen mostly free):

$$\frac{p_{\text{CH}}}{p_{\text{Fe I}}} \propto \frac{A^{4/3}}{B} , \qquad \frac{p_{\text{CN}}}{p_{\text{Fe I}}} \propto \frac{A^{4/3}}{B^2} , \qquad \frac{p_{\text{Fe I}}}{p_{H^-}} \propto \frac{1}{A^{2/3}} . \tag{5}$$

If one applies these relations to the data of equations (1) and (3), one finds that star H deviates from the low-velocity giants in terms of the abundance ratios A and B by the following amounts:

$$\text{Case 1:} \quad \Delta \log A = +0.5 , \quad \Delta \log B = +1.0 . \tag{6}$$

$$\text{Case 2:} \quad \Delta \log A = +0.6 , \quad \Delta \log B = +0.4 . \tag{7}$$

In both cases the overdeterminateness (two unknowns, but three data) does not lead to discrepancies exceeding the observational uncertainties.

We conclude that for star H compared to low-velocity giants the value of A is increased, i.e., the abundance of the metals decreased, by a factor of 3 or 4, and that,

similarly, the value of B is increased, i.e., the abundance of the oxygen decreased, by a factor somewhere between 2.5 and 10.

This result may be compared with that of an earlier spectroscopic comparison between high- and low-velocity F dwarfs (Schwarzschild 1950), which led in the present terms to the following conclusion:

$$\text{F dwarfs:} \qquad \Delta \log \frac{A}{B} = +0.4 . \tag{8}$$

Comparison of this result for the F dwarfs with the alternative results of equations (6) or (7) for the K giants suggests that case 2 rather than case 1 is relevant for star H, in agreement with the conclusion indicated above.

One further conclusion can be drawn from the as yet unused datum of equation (2). This datum shows directly that star H does not deviate significantly from the low-velocity giants in the abundance of barium and several rare earths as a group, relative to iron. This observation may become of interest for the theory of the origin of the heavier elements, since processes are frequently proposed for the origin of the very heavy elements which differ from those proposed for the elements of the iron peak.

We may summarize the results as follows: the high-velocity giant star H deviates from the low-velocity giants in having a lower metal abundance by approximately a factor of 4 and a lower abundance of the oxygen group by a similar, but possibly somewhat smaller, factor. Similar deviations, though of a smaller amount, appear to hold for the high-velocity giant stars Q and K. No deviations were observed for stars L, M, and I. None of the high-velocity giants deviates significantly from the low-velocity giants in the abundance of the heaviest elements relative to iron.

Although this investigation appears to have led to positive results, the work involved has seemed proportionately very large. The efficiency of future similar investigations might be increased by two changes. First, a smaller number of program stars could be used if their selection were based not on velocity but on spectroscopic criteria detectable from medium-dispersion spectra or from narrow-band photoelectric measurements. Second, the reduction of the number of program stars would make it practicable to take much wider spectrograms and thereby to reach a higher accuracy for the same amount of labor in measuring and reduction.

We would like to thank J. Schopp for the color measurements he made for this investigation and J. Rogerson, D. Lautman, and R. Howard for their extensive help in this program. We record with sincere gratitude that this investigation would not have been possible without the generosity of the Mount Wilson Observatory and the persistent help and advice from its staff.

REFERENCES

Aller, L H., and Chamberlain, J W. 1951, *Ap. J.*, **114**, 52.
Bell, B. 1951, *Special Rept* , No. 35, Harvard University.
Burbidge, G. and E 1956, *Ap. J.*, **124**, 116.
Davis, D. N. 1947, *Ap J.*, **106**, 28.
Gratton, L. 1953, *5. Colloque International d'Astrophysique à Liége: Les Processus nucléaires dans les astres*, p. 419
Iwanowska, W. 1950, *Bull. Astr Obs Torun*, No. 9, p. 25.
Johnson, H. L., and Morgan, W. W. 1953, *Ap J.*, **117**, 313.
Koelbloed, D. 1953, *Pub Astr. Inst Amsterdam*, No. 10
Miczaika, G. R. 1950, *Zs f. Ap* , **27**, 1
Roman, N. G 1952, *Ap. J.*, **116**, 135.
———. 1955, *Ap. J. Suppl.*, No. 18.
St. John, C. E., *et al.* 1928, *Revised Rowland Table of Solar Spectrum* ("Publications of the Carnegie Institution of Washington," No 396 [Washington: Carnegie Institution of Washington]).
Schwarzschild, M and B. 1950, *Ap. J.*, **112**, 248.
Schwarzschild, M., Searle, L , and Howard, R. 1955, *Ap J.*, **122**, 353.
Schwarzschild, M., Spitzer, L., Jr., and Wildt, R. 1951, *Ap. J.*, **114**, 398.